RESEARCH ARTICLE

A Sensitivity-Driven Inversion Framework for Efficient Calibration of 3D Geomechanical Models: Application to a Shale Reservoir

Hao Wu[1,2,*], **Xinrui Lyu**[1,2], **Xiaofei Shang**[1,2], **Xiaokai Huang**[3] and **Yanhai Chang**[4]

[1] National Energy Shale Oil Research and Development Center, Beijing 102206, China
[2] SINOPEC Petroleum Exploration and Production Research Institute, Beijing 102206, China
[3] Petroleum Engineering Technology Research Institute, Sinopec Jiangsu Oilfield Company, Yangzhou 225009, China
[4] State Key Laboratory of Digital Intelligent Technology for Unmanned Coal Mining, Anhui University of Science and Technology, Huainan 232001, China

Abstract

Accurate in-situ stress characterization is essential for hydraulic fracturing design in shale reservoirs, yet 3D geomechanical model calibration still relies on iterative trial-and-error procedures that are computationally intensive and physically opaque. Sensitivity analysis, though widely used to evaluate the influence of elastic parameters, is typically treated as descriptive rather than predictive. This work proposes a sensitivity-driven inversion framework for efficient calibration of horizontal stresses in 3D geomechanical models. Controlled perturbation simulations on a baseline model quantify the responses of maximum and minimum horizontal stresses (S_H and S_h) to variations in Young's modulus and Poisson's ratio across stratigraphic units. These responses form a sensitivity matrix establishing a first-order relationship between parameter perturbations and stress variations. A dual-objective inversion scheme then simultaneously constrains S_H and S_h, enabling direct single-step parameter estimation and reducing reliance on iterative calibration. Application to a shale reservoir shows good agreement with reference stress profiles, with interval-averaged deviations reduced below 1%. Moreover, sensitivity relationships from a reference block serve as a first-order approximation for calibrating geologically similar neighboring blocks, demonstrating cross-block transfer potential. The framework offers an efficient, physically interpretable stress calibration approach and provides a practical alternative to conventional empirical methods.

Keywords: shale reservoir, geomechanical modeling, in-situ stress, sensitivity analysis, parameter inversion, cross-block transfer.

Submitted: 23 April 2026
Revised: 28 July 2026
Accepted: 30 July 2026
Published: 08 August 2026

Vol. 2, **No.** 3, 2026.
10.62762/RS.2026.836628

***Corresponding author:**
Hao Wu
haowucn@outlook.com

Citation
Wu, H., Lyu, X., Shang, X., Huang, X., & Chang, Y. (2026). A Sensitivity-Driven Inversion Framework for Efficient Calibration of 3D Geomechanical Models: Application to a Shale Reservoir. *Reservoir Science*, 2(3), 305–323.

1 Introduction

Shale oil development has expanded rapidly over the past two decades, largely driven by the integration of horizontal drilling and multi-stage hydraulic fracturing technologies [1–4]. In China, continental lacustrine shale oil systems have been extensively characterized in terms of their formation mechanisms, geological features, and development potential [5–7]. Unlike conventional reservoirs where matrix permeability governs productivity, shale oil recovery critically depends on the geometry, connectivity, and complexity of the induced fracture networks [8–10]. The initiation pressure, fracture propagation path, vertical containment, and stimulated reservoir volume are fundamentally controlled by the in-situ stress state [11–13]. Recent multiscale geomechanical and reservoir studies further emphasize that accurate 3D stress prediction is essential for stimulation efficiency and long-term production forecasting [14, 15]. As a result, constraining the three-dimensional stress field has become a key task in shale oil development.

However, stress fields in shale-bearing basins are often far from uniform due to complex tectonic evolution, strong lithologic heterogeneity, and spatial variations in mechanical properties between adjacent formations [16, 17]. Interbedded brittle–ductile alternations, lamina-scale variability, and structural discontinuities further complicate fracture design and flow prediction. Traditional one-dimensional stress estimation methods provide reasonable wellbore-scale stress estimates [18, 19]. Yet they implicitly assume vertical equilibrium and lateral homogeneity, limiting their applicability in laterally heterogeneous lacustrine shale systems. They also fail to incorporate mechanical feedback from surrounding formations, which have been increasingly recognized as non-negligible controls in recent geomechanical studies [20].

In contrast, three-dimensional geomechanical modeling has evolved into a more rigorous and comprehensive framework capable of integrating seismic interpretation, well logs, core testing, microseismic monitoring, and discrete fracture data [20, 21]. Such models have enabled spatially continuous stress prediction across reservoirs and their bounding formations, and have proven effective in evaluating fracture containment, stress barriers, reactivation potential, and geohazard risks [22, 23].

A key remaining challenge for 3D geomechanical modeling is quantifying how elastic properties (particularly Young's modulus (YM) and Poisson's ratio (PR)) govern the redistribution of the principal stresses. Numerous laboratory and modeling studies have shown that small variations in elastic parameters can lead to significant changes in S_H and S_h [24, 25]. Furthermore, recent experimental investigations have demonstrated that mineralogical variations, organic matter content, and pore-fluid interactions can significantly modify shale elastic properties [26–30], adding further uncertainty to stress prediction. However, the relative importance of elastic contrasts within different stratigraphic intervals (overburden, underburden, sideburden, and the reservoir itself) are insufficiently documented, particularly in lacustrine shale systems with strong mechanical heterogeneity. A systematic, layer-by-layer sensitivity analysis is therefore needed for both 3D geomechanical model calibration and operational decision-making. In addition, recent studies on dynamic stress evolution in fractured shale reservoirs further underscore the sensitivity of in-situ stress states to variations in formation mechanical properties [31, 32]. Moreover, systematic workflows for building and calibrating 3D geomechanical models have been proposed, yet they still rely heavily on iterative manual adjustment [33].

The Gaoyou Sag in the Subei Basin represents a typical shale oil system characterized by lacustrine deposition, tectonic deformation, and significant mechanical heterogeneity [34]. The target F_2 member comprises 230–300 m of dark shale interbedded with variable-strength lithologies [35], forming multiple fault-block compartments trending NEE–SWW [36]. Previous studies in this area have focused on stratigraphic architecture, facies distribution, and oil enrichment patterns [37]. However, recent work has highlighted the need for integrated petrophysical–geomechanical evaluation in lacustrine shale reservoirs [14, 20], and comprehensive 3D geomechanical modeling combined with elastic sensitivity analysis remains lacking.

To address these limitations, this study develops a sensitivity-driven inversion framework for the calibration of horizontal stresses in 3D geomechanical models. Rather than relying on iterative adjustments, the proposed approach establishes an explicit relationship between rock mechanical parameters and stress responses via a sensitivity matrix derived from controlled perturbation simulations. On this basis, a dual-objective inversion scheme is formulated to simultaneously constrain S_H and S_h. The framework is further extended by introducing a cross-block sensitivity transfer strategy, which allows previously

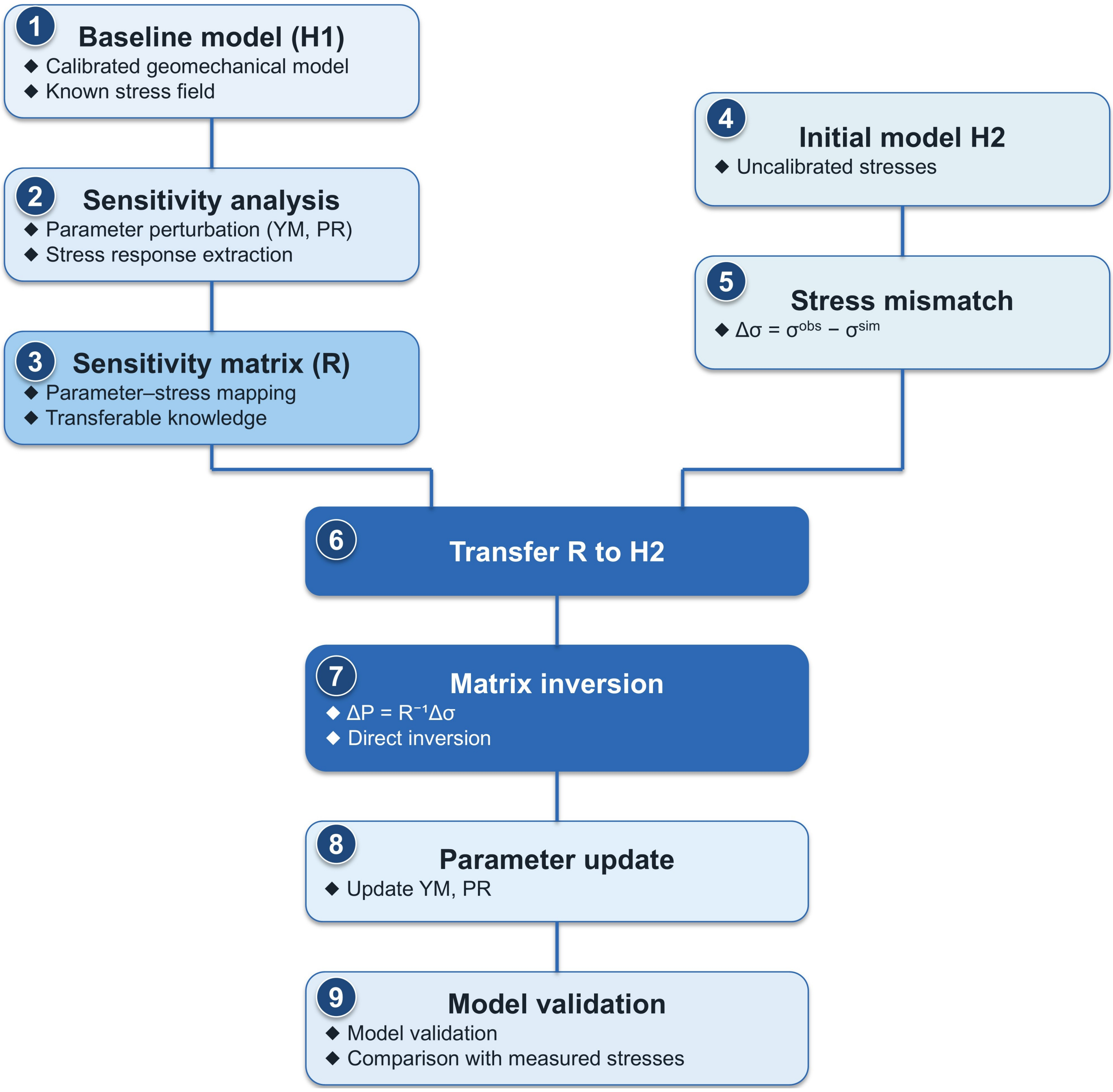

Figure 1. Overall workflow of the proposed framework.

derived sensitivity relationships to be reused in geologically similar areas. The key contributions of this work are threefold: (1) the development of a sensitivity-driven inversion framework that replaces empirical calibration; (2) the introduction of an adaptive elastic parameter selection strategy based on sensitivity dominance and data constraints; (3) the proposal of a cross-block sensitivity transfer strategy for improving calibration efficiency in geologically comparable areas. The method is demonstrated using a shale reservoir case, with a focus on both calibration accuracy and computational efficiency.

2 Theoretical Framework and Methodology

In conventional 3D geomechanical modeling, calibration is commonly performed through iterative trial-and-error adjustment of regional stress gradients or local elastic parameters until the simulated stresses match single-well observations. Although this approach may improve the local fitting quality, it is computationally expensive and may compromise the physical consistency of the regional stress field, particularly when boundary stresses are repeatedly modified to satisfy local stress data. To address these limitations, this study proposes a sensitivity-driven inversion framework for efficient calibration of 3D geomechanical models (Figure 1). The framework is built on three key ideas: (1) the physical decoupling of vertical stress and horizontal stresses; (2) the quantification of elastic parameter–stress relationships through sensitivity analysis; (3) the direct estimation of elastic parameter updates through matrix-based inversion.

2.1 Mechanistic Decoupling of Vertical and Horizontal Stresses

A prerequisite for efficient inversion is to distinguish which stress components can be treated as known quantities and which require calibration. In layered sedimentary systems, the in-situ stress field can be separated into vertical stress and horizontal stresses according to their governing mechanisms.

The vertical stress S_v (MPa) is assumed to be primarily controlled by gravitational loading and can be calculated by integrating the density profile from the surface to depth z:

$$S_v(z) = \int_0^z \rho(\xi) g \, d\xi \tag{1}$$

where $\rho(\xi)$ is the bulk density (kg/m^3) at depth ξ (m), and g is the gravitational acceleration (9.81 m/s^2).

Because S_v is directly determined by the overlying rock mass and is generally well constrained by density logs, it is treated as a known input to the geomechanical model rather than an inversion target. This treatment is widely used in reservoir geomechanics [38, 39] and provides a relatively robust vertical stress constraint.

In contrast, the maximum and minimum horizontal principal stresses, denoted as S_H (MPa) and S_h (MPa), are influenced by both far-field tectonic loading and local elastic interactions among stratigraphic units. For a linear elastic medium, the stress–strain relationship can be written in generalized form as:

$$\sigma = C\varepsilon \tag{2}$$

where σ is the stress tensor, ε is the strain tensor, and C is the constitutive stiffness matrix determined by the elastic parameters of the rock mass.

This implies that changes in YM (GPa) and PR in surrounding formations may alter the local redistribution of horizontal stresses through elastic coupling, even when the far-field boundary condition remains unchanged. Therefore, the calibration problem addressed in this study is reduced to the adjustment of S_H and S_h, while keeping S_v fixed. This mechanistic decoupling not only simplifies the inversion problem but also helps preserve the physical clarity of the calibration procedure.

2.2 Sensitivity Quantification of Elastic Parameters

To convert qualitative mechanical understanding into a quantitative inversion basis, a control-variable sensitivity analysis is performed on a calibrated baseline model. The objective is to quantify how perturbations in elastic parameters of the surrounding formations affect the horizontal stresses within the reservoir.

Let P_j denote the j-th mechanical parameter to be perturbed. In this study, P_j may represent YM or PR of the overburden or underburden, depending on the selected inversion setting. A relative perturbation is applied as:

$$P_j' = P_j(1 + \delta_j) \tag{3}$$

where P_j' is the perturbed value and δ_j is the imposed relative perturbation ratio. In practical calculations, δ_j is typically chosen within a moderate range, such as $\pm 10\%$, $\pm 20\%$, or an equivalent fixed increment, so that the resulting stress response remains approximately linear.

For each perturbation run, all other parameters are kept unchanged, and the average horizontal stresses in the reservoir are extracted from the simulation results. The average relative stress variation induced by perturbation of elastic parameter P_j is defined as:

$$\Delta S_H^{(j)} = \frac{S_{H,avg}^p - S_{H,avg}^0}{S_{H,avg}^0} \tag{4}$$

$$\Delta S_h^{(j)} = \frac{S_{h,avg}^p - S_{h,avg}^0}{S_{h,avg}^0} \tag{5}$$

where $S_{H,avg}^0$ and $S_{h,avg}^0$ are the average horizontal stresses (MPa) in the baseline model, and $S_{H,avg}^p$ and $S_{h,avg}^p$ are the corresponding stresses (MPa) in the perturbed model.

The sensitivity coefficients are then defined as the stress response per unit elastic parameter perturbation:

$$R_{H,j} = \frac{\Delta S_H^{(j)}}{\delta_j} \tag{6}$$

$$R_{h,j} = \frac{\Delta S_h^{(j)}}{\delta_j} \tag{7}$$

where $R_{H,j}$ and $R_{h,j}$ represent the sensitivity coefficients of S_H and S_h, respectively. The sign of the sensitivity coefficient represents the direction of stress response. A negative value indicates that increasing the elastic parameter causes a reduction in the corresponding horizontal stress.

The above sensitivity analysis forms the quantitative basis for subsequent matrix construction. More importantly, it enables the identification of dominant controlling layers, which is later used to guide adaptive elastic parameter selection in the inversion stage. The selection of adjustable parameters was not intended to represent a unique inversion of all possible geological uncertainties. Instead, it follows a sensitivity-guided parameter reduction strategy. Parameters with stronger stress influence and relatively larger uncertainty were selected, while parameters with stronger geological constraints were kept unchanged to reduce inversion non-uniqueness.

2.3 Sensitivity Matrix Construction

Once the sensitivity coefficients are obtained, they are assembled into a sensitivity matrix that provides a compact mapping from elastic parameter perturbations to horizontal stress variations. For a general case involving n inversion elastic parameters, define the elastic parameter-update vector as:

$$\Delta P = \begin{bmatrix} \Delta P_1 \\ \Delta P_2 \\ \vdots \\ \Delta P_n \end{bmatrix} \tag{8}$$

Define the stress-response vector as:

$$\Delta \sigma = \begin{bmatrix} \Delta S_H \\ \Delta S_h \end{bmatrix} \tag{9}$$

Then the first-order linear relationship between stress variations and elastic parameter perturbations can be written as:

$$\Delta \sigma = R \Delta P \tag{10}$$

where R is the sensitivity matrix:

$$R = \begin{bmatrix} R_{H,1} & R_{H,2} & \cdots & R_{H,n} \\ R_{h,1} & R_{h,2} & \cdots & R_{h,n} \end{bmatrix} \tag{11}$$

The matrix R describes the linearized elastic parameter–stress coupling around the baseline model. In this study, the matrix is constructed from the sensitivity analysis results of a mature reference block and is later used as a candidate first-order calibration operator for a neighboring target block.

When the mechanical properties of the overburden are well constrained by logging data or laboratory measurements, only the underburden elastic parameters are selected as inversion targets. In this case, the elastic parameter vector (Equation 8) becomes:

$$\Delta P_u = \begin{bmatrix} \Delta YM_u \\ \Delta PR_u \end{bmatrix} \tag{12}$$

where ΔYM_u and ΔPR_u represent the relative perturbation ratios of YM and PR in the underburden, respectively. The corresponding reduced sensitivity matrix (Equation 11) is:

$$R_u = \begin{bmatrix} R_{H,YM_u} & R_{H,PR_u} \\ R_{h,YM_u} & R_{h,PR_u} \end{bmatrix} \tag{13}$$

where R_{H,YM_u} and R_{H,PR_u} represent the sensitivity coefficients of S_H with respect to YM_u and PR_u, respectively, R_{h,YM_u} and R_{h,PR_u} represent the sensitivity coefficients of S_h to YM_u and PR_u, respectively.

2.4 Dual-objective Inversion Algorithm

In the target block, the initial geomechanical model yields simulated horizontal stresses that may differ from observed values. Define the stress mismatch vector as:

$$\Delta \sigma = \begin{bmatrix} (S^{obs}_{H,avg} - S^{sim}_{H,avg})/S^{obs}_{H,avg} \\ (S^{obs}_{h,avg} - S^{sim}_{h,avg})/S^{obs}_{h,avg} \end{bmatrix} \tag{14}$$

where $S^{obs}_{H,avg}$ and $S^{obs}_{h,avg}$ represent the average reference horizontal stress profiles established from integrated geomechanical interpretation, $S^{sim}_{H,avg}$ and $S^{sim}_{h,avg}$ are the average simulated stresses from the initial model. The minimum horizontal principal stress S_h is constrained by hydraulic-fracturing measurements, whereas the continuous stress profiles are obtained from log-based geomechanical calculations calibrated against available field measurements. The maximum horizontal principal stress S_H is estimated from the calibrated one-dimensional geomechanical model using elastic properties, pore pressure, and regional tectonic constraints.

The inversion problem is to find the elastic parameter correction vector ΔP such that:

$$R \Delta P \approx \Delta \sigma \tag{15}$$

When the number of unknown parameters equals two, such as in the reduced-parameter underburden-only setting, the solution can be directly obtained through matrix inversion:

$$\begin{bmatrix} \Delta YM_u \\ \Delta PR_u \end{bmatrix} = R_u^{-1} \begin{bmatrix} (S_{H,avg}^{obs} - S_{H,avg}^{sim})/S_{H,avg}^{obs} \\ (S_{h,avg}^{obs} - S_{h,avg}^{sim})/S_{h,avg}^{obs} \end{bmatrix} \quad (16)$$

$$S_{k,avg}^{m} = \frac{1}{N}\sum_{i=1}^{N} S_{k,i}^{m} \quad (17)$$

where $k = H, h, m = obs, sim$, N denotes the number of depth points or grid cells within the reservoir interval.

After the parameter corrections are obtained, the updated parameters are:

$$P_j^{new} = P_j^{old}(1 + \Delta P_j) \quad (18)$$

2.5 Adaptive Parameter Selection Strategy

A key practical issue in inversion is deciding which parameters should be included as unknowns. Including too many parameters may increase non-uniqueness and reduce interpretability, whereas excluding important parameters may lead to biased calibration. To address this trade-off, an adaptive elastic parameter selection strategy is introduced. The strategy is guided by two principles:

1. Sensitivity dominance: elastic parameters associated with formations that exert stronger control on S_H and S_h should be prioritized.
2. Data constraint level: elastic parameters that are already well constrained by measurements should preferably be fixed.

In many practical shale reservoir cases, including the case study presented in this work, the overburden properties are treated as fixed inputs because they are already tightly constrained by high-confidence logging data. By contrast, the underburden extends well below the reservoir and is often poorly constrained, especially when no deep logging or core measurements are available. If the sensitivity analysis further indicates that the underburden exerts the dominant control on horizontal stress redistribution, then it is both physically reasonable and mathematically advantageous to adopt the reduced-parameter underburden-only inversion. Under this setting, the inversion target is:

$$\Delta P = \Delta P_u = \begin{bmatrix} \Delta YM_u \\ \Delta PR_u \end{bmatrix} \quad (19)$$

However, the framework is not restricted to this case. If the overburden mechanical properties are uncertain or lack sufficient measurements, the inversion can be expanded to jointly update overburden and underburden properties:

$$\Delta P = \Delta P_{ou} = \begin{bmatrix} \Delta YM_o \\ \Delta PR_o \\ \Delta YM_u \\ \Delta PR_u \end{bmatrix} \quad (20)$$

To ensure physically meaningful results, elastic parameter updates are constrained within reasonable geological intervals:

$$P_j^{min} \le P_j^{new} \le P_j^{max} \quad (21)$$

where P_j^{min} and P_j^{max} denote the lower and upper bounds determined from logging interpretation, laboratory measurements, or regional geological knowledge.

2.6 Cross-block Sensitivity Transfer Strategy

The central idea of cross-block sensitivity transfer is that sensitivity coefficients characterize the local parameter–stress response of the baseline model governed by stratigraphic architecture, lithological combinations, and the regional tectonic stress regime. Therefore, for neighboring or geologically analogous blocks, the sensitivity matrix derived from a calibrated reference block may remain approximately valid and can be reused for efficient calibration of a target block.

Suppose Block 1 is a mature reference block where a calibrated baseline model has already been established, and the sensitivity matrix $\mathbf{R}^{(1)}$ has been obtained. For a target Block 2 with similar geological conditions, the same matrix may be used as a first-order approximation:

$$\mathbf{R}^{(2)} \approx \mathbf{R}^{(1)} \quad (22)$$

Under this assumption, for the directly invertible reduced-parameter case, the inversion in Block 2 becomes:

$$\Delta \mathbf{P}^{(2)} = \left(\mathbf{R}^{(1)}\right)^{-1} \Delta\sigma^{(2)} \quad (23)$$

This transfer strategy may reduce the need to repeat the full perturbation analysis during preliminary calibration of geologically comparable blocks. Its validity relies on geological similarity between the reference and target blocks, particularly in terms of stratigraphic configuration, lithological assemblage, and tectonic loading mechanism.

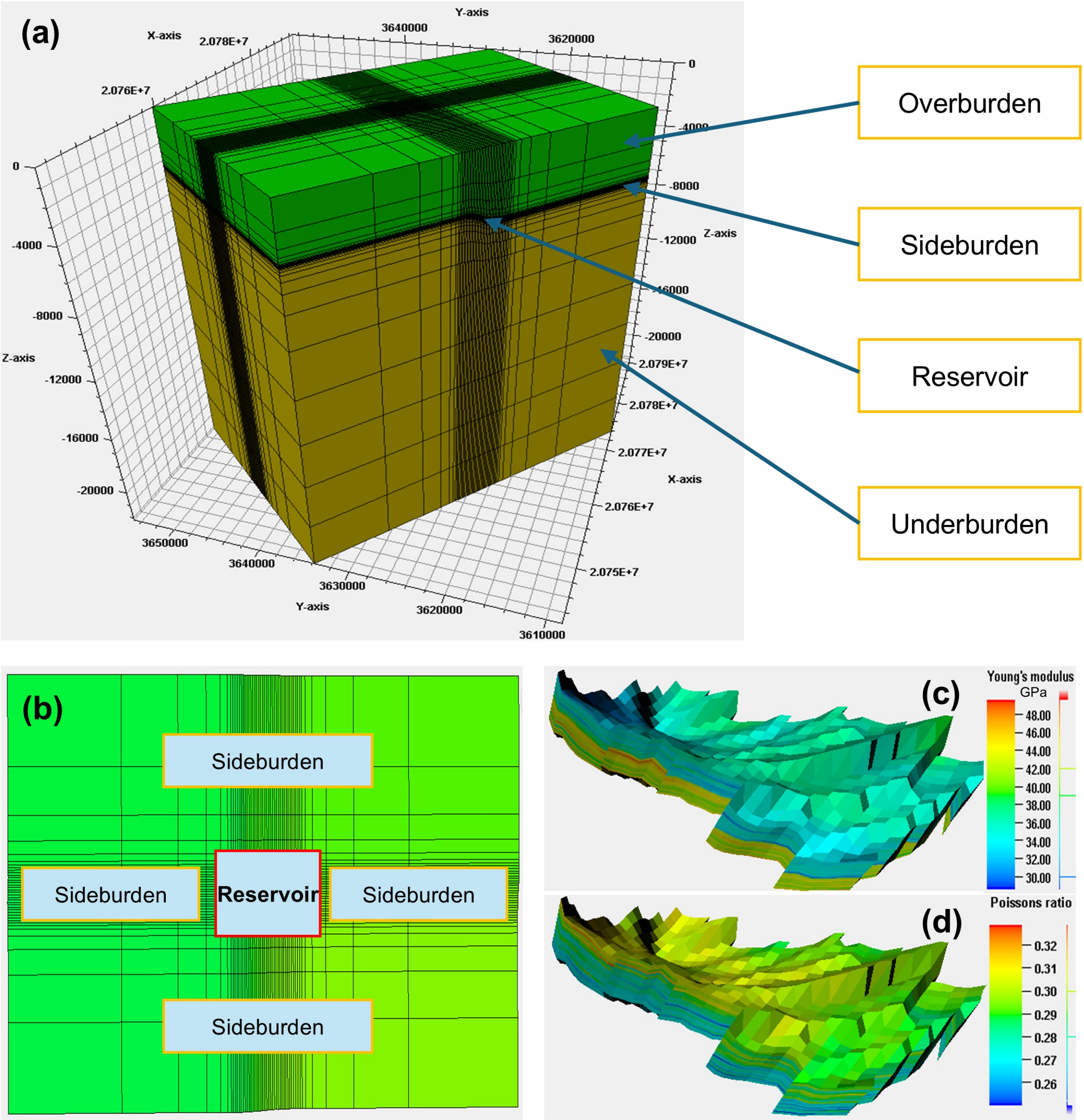

Figure 2. Schematic of the 3D geomechanical model, showing: (a) the vertical distribution of the overburden, sideburden, underburden, and reservoir; (b) the lateral distribution of the sideburden and reservoir; and (c, d) the distributions of Young's modulus and Poisson's ratio within the reservoir, respectively.

3 Establishment of Prior Knowledge: the Baseline Study

To implement the proposed framework, the dominant mechanical controls must first be identified and quantified within a mature baseline block. Block H1, located in the Gaoyou Sag of the Subei Basin, was selected for this purpose. The target F_2 member contains 230–300 m of lacustrine shale, characterized by NEE-trending fault blocks and a dominant S_H direction of approximately N45°E. A high-fidelity baseline model was constructed and validated against single-well measurements, achieving an average relative error below 1%.

3.1 Baseline Model Setup

A baseline 3D geomechanical model is established in a reference block (Block H1) to provide the prior knowledge required for the proposed

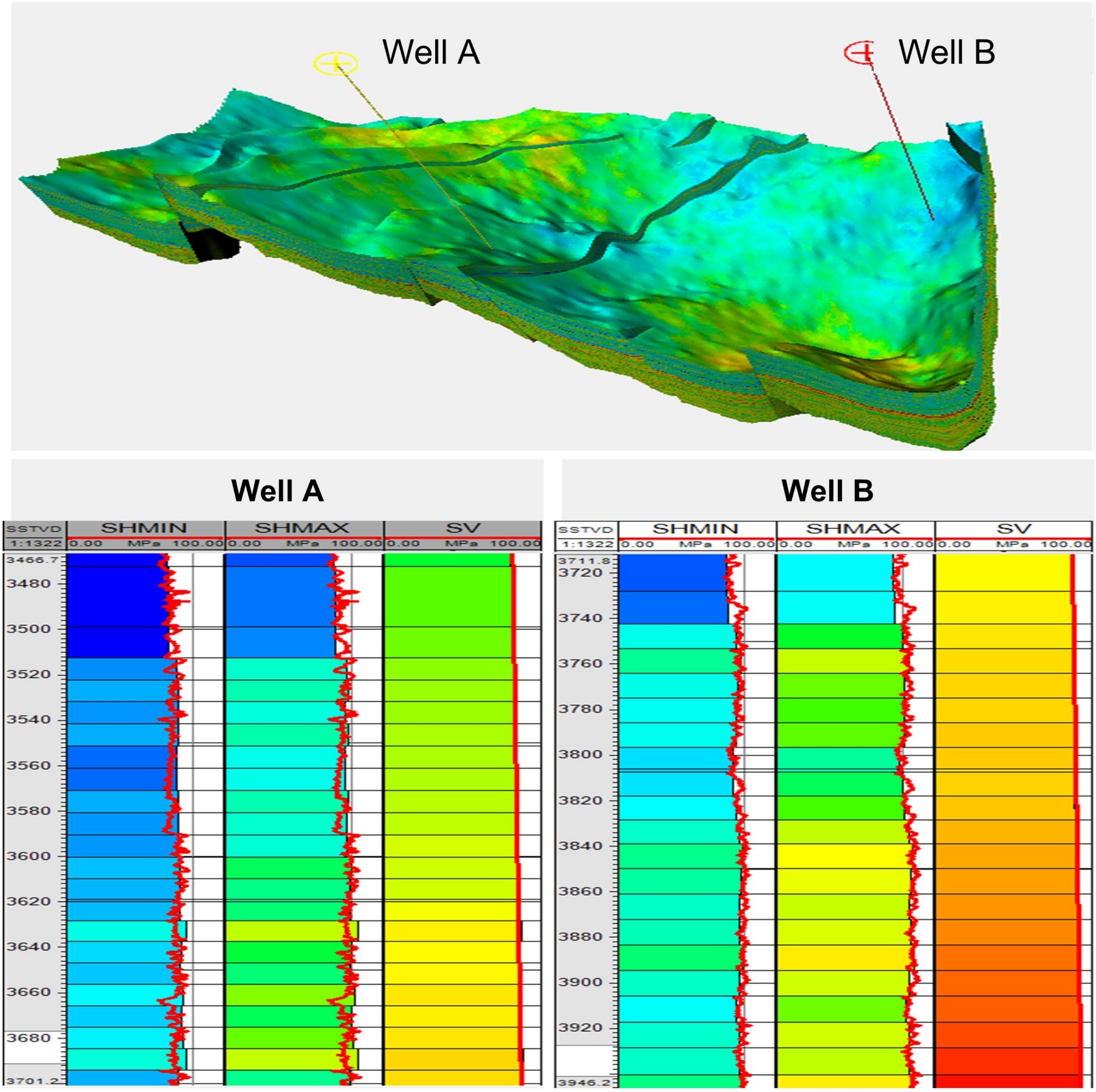

Figure 3. Validation of baseline 3D geomechanical model based on the single-well data, where the red curves represent the log-derived reference stress profiles constrained by available field measurements, whereas the colored blocks represent the corresponding stresses extracted from the 3D geomechanical model.

sensitivity-driven inversion framework. The geological model is constructed based on integrated interpretation of 3D seismic data and well logs. The target interval consists of interbedded shale and silty layers, characterized by strong vertical heterogeneity and relatively continuous lateral distribution. The model domain is discretized into four mechanical units: reservoir, overburden, underburden, and sideburden (Figure 2).

The reservoir properties are derived from logging interpretation and 3D property modeling, and are treated as fixed inputs in the sensitivity analysis. The surrounding formations are assigned initial elastic properties based on available geological and petrophysical information.

The vertical stress S_v is calculated using density integration (Equation 1), while the horizontal stresses are initialized using regional stress gradients. The boundary conditions were designed to reproduce the regional tectonic stress environment. Gravity loading was applied based on the three-dimensional density distribution, while horizontal tectonic stresses were imposed according to the regional stress gradients and stress orientation derived from available regional stress constraints. The same boundary-condition strategy was adopted for Blocks H1 and H2 to ensure consistency during cross-block calibration. The baseline model is calibrated using available stress measurements (e.g., mini-frac tests or log-derived stresses) to ensure that the simulated stress field reasonably represents in-situ conditions (Figure 3). This calibrated baseline model serves as the foundation for subsequent sensitivity analysis and matrix construction.

3.2 Sensitivity hierarchy of surrounding formations

Based on the baseline model, a series of controlled perturbation simulations are performed to quantify the influence of elastic parameters in different stratigraphic units on reservoir horizontal stresses (Figures 4, 5, 6, and 7).

For each formation (overburden, underburden, sideburden), YM and PR are perturbed individually while keeping other parameters constant. The resulting variations in S_H and S_h are extracted and analyzed (Figures 5 and 7). The results reveal a consistent sensitivity hierarchy: (1) the **underburden** exerts the strongest control on both S_H and S_h; (2) the **overburden** has a secondary effect; (3) the **sideburden** has minimal influence.

This hierarchy is consistently observed across different perturbation magnitudes and parameter types, suggesting that it is not an artifact of a specific perturbation scenario but rather reflects the modeled mechanical response of the system. The dominant role of underburden can be attributed to its relatively large thickness and greater capacity to accumulate and redistribute elastic strain energy. In contrast, the limited influence of the sideburden indicates that lateral stress transfer contributed less to the interval-averaged reservoir stress response compared with vertical mechanical interactions under the investigated perturbation scenarios.

3.3 Quantitative Extraction of the Sensitivity Matrix

In this case, the mechanical properties of the overburden are well constrained by logging data. Based on the sensitivity hierarchy and the availability of logging-constrained overburden properties, only the underburden parameters are selected as inversion targets. Using the sensitivity coefficients defined in Equation (6) and (7), the parameter–stress relationships are quantified and assembled into a sensitivity matrix. For the reduced-parameter setting (underburden-only), the sensitivity matrix takes the form:

$$\mathbf{R}_u = \begin{bmatrix} R_{H,YM_u} & R_{H,PR_u} \\ R_{h,YM_u} & R_{h,PR_u} \end{bmatrix} = \begin{bmatrix} 0.15\%/1\% & 0.35\%/1\% \\ 0.12\%/1\% & 0.50\%/1\% \end{bmatrix} \tag{24}$$

Each coefficient in $\mathbf{R}_u$ is calculated by averaging the stress responses over the reservoir interval for the corresponding perturbation case. This expanded matrix is retained as part of the prior knowledge base for potential use in joint inversion scenarios. The resulting sensitivity matrix constitutes a transferable parameter–stress mapping, which encodes the mechanical behavior of the system and forms the core input for the inversion procedure applied in the target block.

4 Case Application: Rapid Calibration via Cross-block Transfer

To validate the efficiency of the framework, the prior sensitivity knowledge was transferred to calibrate the newly developed Block H2, situated approximately 6 km southwest of Block H1. Both blocks share a highly consistent regional tectonic background, lithological sequence, and S_H orientation, providing a reasonable basis for cross-block migration.

4.1 Geological Analogy and Initial Model in Target Block

To validate the proposed framework, the sensitivity matrix derived from the reference block (H1) is applied to a neighboring block (H2). The two blocks share similar geological characteristics. Specifically, they share consistent NEE-trending fault compartmentalization, similar target formation thicknesses, identical regional maximum horizontal stress (S_H) orientation, and comparable interbedded lithological compositions (Figure 8). These similarities provide a reasonable basis for applying the cross-block sensitivity transfer strategy.

An initial 3D geomechanical model is constructed for Block H2 using the same workflow as the baseline model. However, discrepancies are observed between simulated and measured stresses. Specifically, the

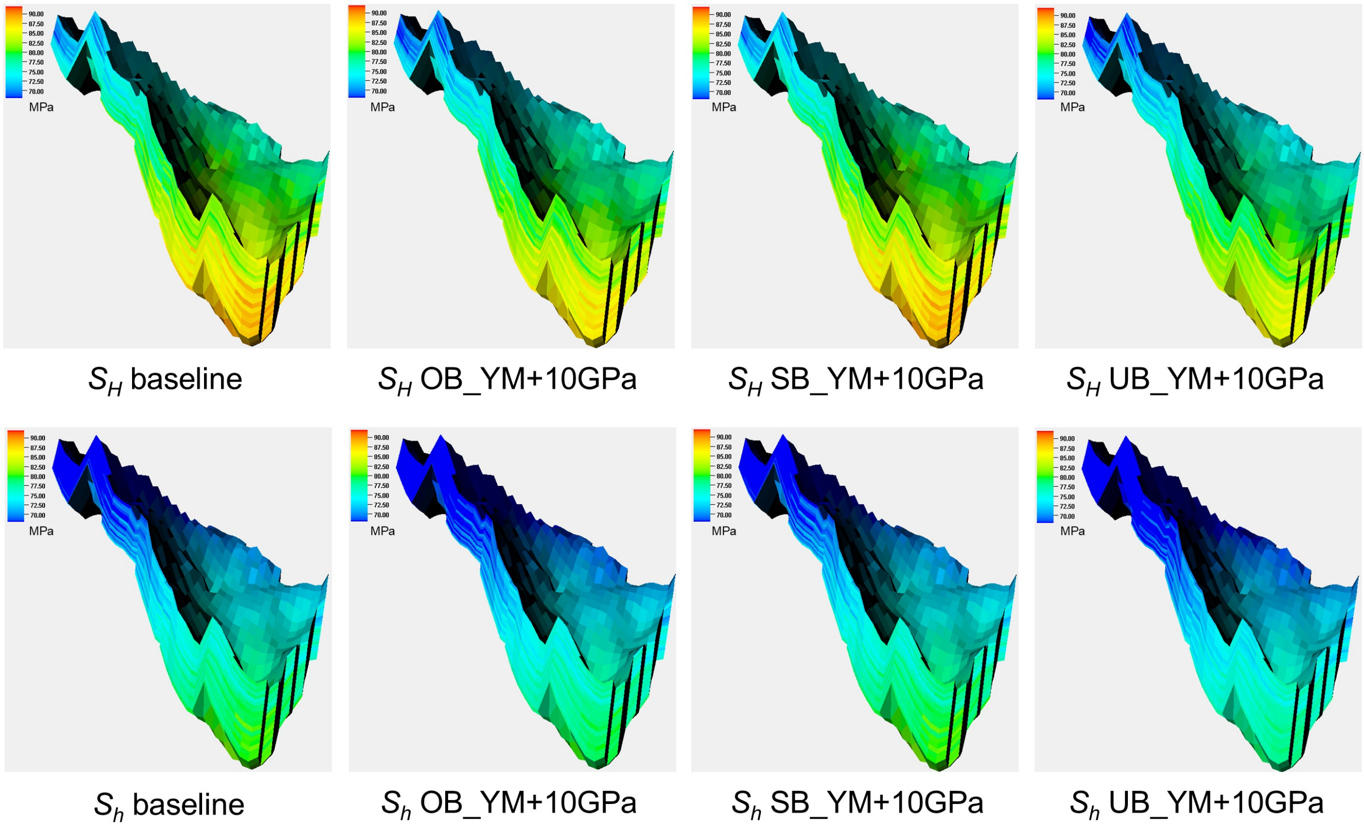

Figure 4. Sensitivity of 3D horizontal stress to Young's modulus, where OB, SB, and UB mean overburden, sideburden, and underburden, respectively.

interval-averaged stress is defined as:

$$S_{k,avg} = \frac{1}{N}\sum_{i=1}^{N} S_{k,i} \tag{25}$$

where $k = H, h$. Here $S^{sim}_{k,avg}$ and $S^{obs}_{k,avg}$ denote the interval-averaged simulated and reference stresses, respectively, as defined in Equation (17). The corresponding relative mismatches between the initial model and the reference are:

$$\Delta S_H = \frac{|S^{sim}_{H,avg} - S^{obs}_{H,avg}|}{S^{obs}_{H,avg}} \times 100\% \approx 3.2\% \tag{26}$$

$$\Delta S_h = \frac{|S^{sim}_{h,avg} - S^{obs}_{h,avg}|}{S^{obs}_{h,avg}} \times 100\% \approx 2.8\% \tag{27}$$

These mismatches indicate that the initial model requires calibration and serves as input to the inversion process. The continuous horizontal stress profiles used for model calibration and error evaluation were generated from one-dimensional well-log-based geomechanical models. The minimum horizontal stress S_h was calibrated using localized field measurements obtained from DFIT tests, whereas the maximum horizontal stress S_H was obtained from a calibrated one-dimensional geomechanical model constrained by elastic properties, pore pressure, and regional stress information.

Therefore, these profiles are treated as reference stress profiles rather than direct measurements.

4.2 Inversion-based Parameter Update

In this case, the mechanical properties of the overburden are relatively well constrained by logging data and are therefore treated as fixed inputs. Based on the sensitivity hierarchy identified in Section 3.2, only the underburden parameters are selected as inversion targets.

The parameter update vector is defined as:

$$\Delta P_u = \begin{bmatrix} \Delta YM_u \\ \Delta PR_u \end{bmatrix} \tag{28}$$

Using the sensitivity matrix R_u, the inversion is performed as:

$$\Delta P_u = R_u^{-1} \cdot \Delta\sigma \tag{29}$$

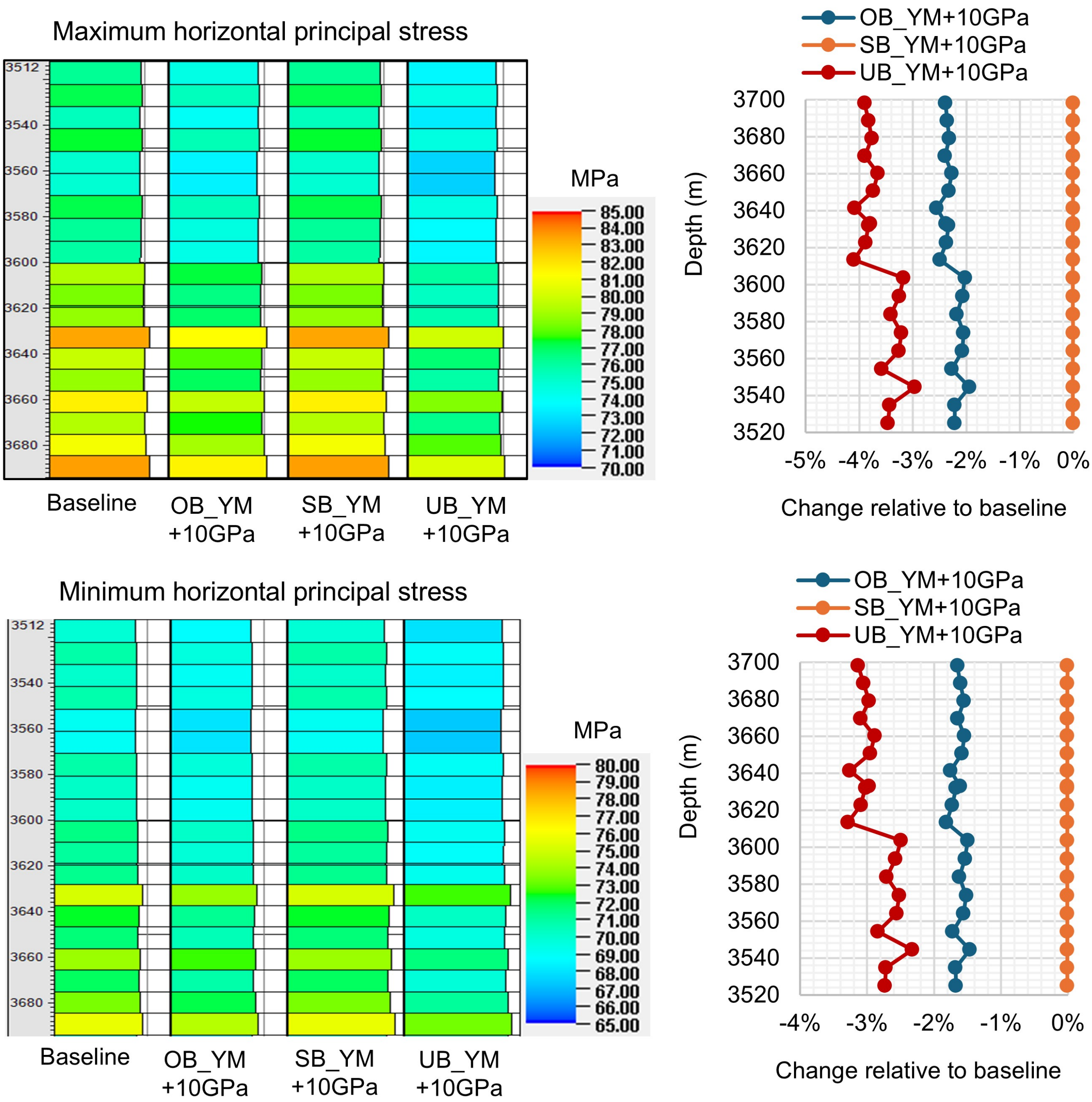

Figure 5. Sensitivity of the single-well horizontal stress profiles to Young's modulus, where OB, SB, and UB mean overburden, sideburden, and underburden, respectively.

The inversion results indicate that an effective reduction of approximately 19% in the underburden YM is required to minimize the horizontal stress mismatch under the current model parameterization. This update represents an effective calibration parameter rather than a unique determination of the actual underburden mechanical property. The inverted PR correction is approximately -1% (a slight reduction), indicating that the stress mismatch is mainly compensated by adjusting YM under the adopted two-parameter inversion framework. This result is consistent with the sensitivity matrix (Equation 24), which shows that S_H and S_h are more sensitive to YM perturbations than to PR perturbations in the underburden of the studied area. Consequently, a larger YM correction is required to close the stress mismatch, while the PR adjustment remains minor.

4.3 Model Update and Validation

The updated parameters are assigned to the geomechanical model, and a new forward simulation is performed (Figure 9). The recalculated stress

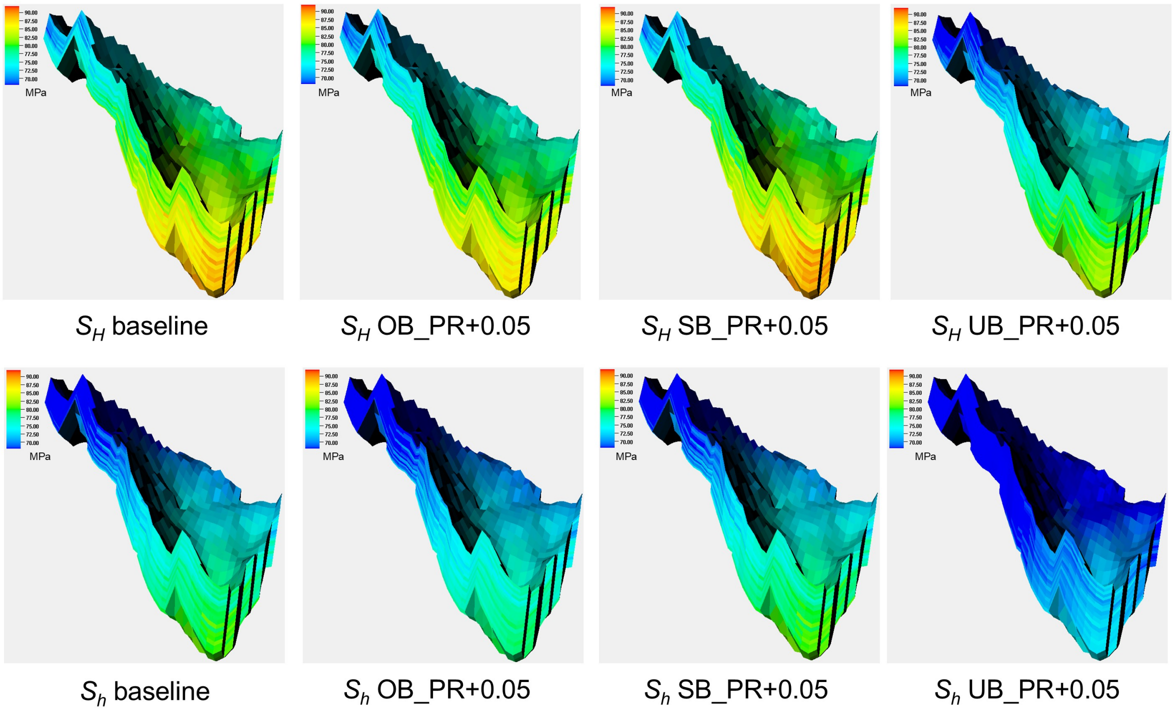

Figure 6. Sensitivity of 3D horizontal stress to Poisson's ratio, where OB, SB, and UB mean overburden, sideburden, and underburden, respectively.

profiles show reduced residuals relative to the reference stress profiles (Figure 10). After calibration, the interval-averaged horizontal stresses showed significantly improved agreement with the reference values, with relative deviations reduced to below 1%. Calibration accuracy was evaluated based on the interval-averaged horizontal stresses within the target reservoir interval. Specifically, the average simulated stress and reference stress were first calculated over the evaluation interval, and the relative mismatch was then quantified (Equations 25-27).

It is worth noting that the calibration is achieved using a single inversion step and one forward simulation, whereas conventional trial-and-error methods typically require multiple iterations. This indicates that the proposed method can effectively reduce computational effort while maintaining acceptable accuracy. This reduction in computational cost is particularly beneficial in multi-well or multi-block modeling scenarios, where repeated calibration is often required.

5 Discussion

5.1 Mechanism-driven Calibration Versus Empirical Tuning

In conventional geomechanical modeling workflows, calibration is often achieved through empirical adjustment of boundary stress conditions or stress gradients until a reasonable match with measured data is obtained. While such approaches may improve local agreement, they may introduce inconsistencies in the spatial distribution of stresses, especially when regional boundary conditions are modified primarily to fit single-well observations.

In contrast, the method proposed in this study is based on a mechanism-driven framework, in which stress calibration is achieved by adjusting elastic parameters of surrounding formations. From a mechanical perspective, horizontal stresses are governed not only by far-field tectonic loading but also by elastic interactions between stratigraphic units. Therefore, modifying effective elastic properties provides a mechanically interpretable calibration pathway while preserving the prescribed boundary-loading pattern.

This distinction is important because it helps maintain consistency with the prescribed regional loading conditions. Instead of forcing the model to match observations through boundary adjustments, the proposed method identifies parameter corrections that naturally lead to the observed stress state. As a result, the calibration process becomes both more interpretable and more reproducible.

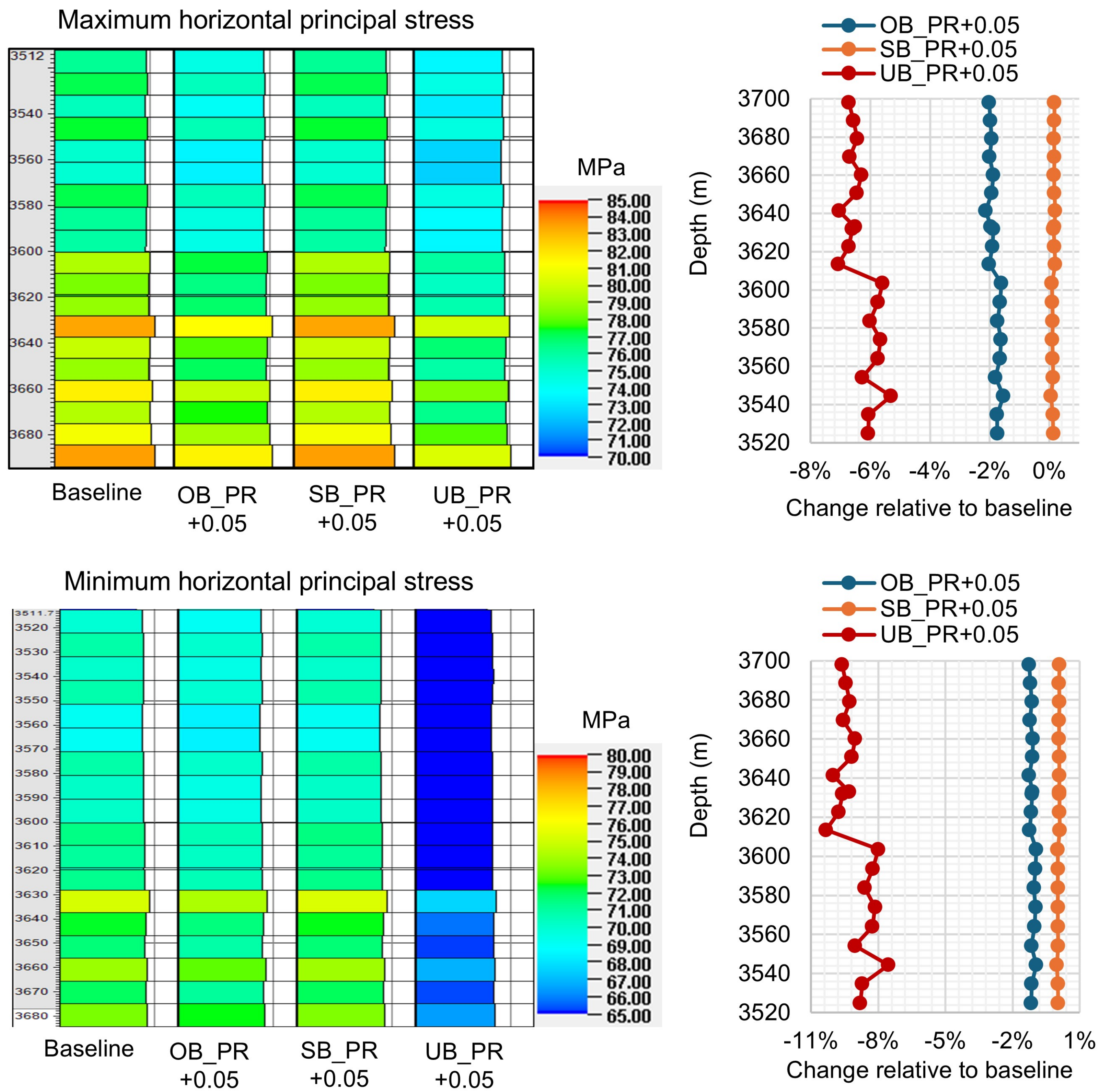

Figure 7. Sensitivity of the single-well horizontal stress profiles to Poisson's ratio, where OB, SB, and UB mean overburden, sideburden, and underburden, respectively.

5.2 Physical Origin of Sensitivity Hierarchy

One of the key observations in this study is the dominant influence of the underburden on reservoir horizontal stresses. This sensitivity hierarchy emerges consistently from the perturbation analysis and is not imposed as an assumption.

The physical origin of this phenomenon can be understood in terms of elastic strain energy distribution and stress transmission pathways. In layered systems, thicker and mechanically continuous units tend to play a more significant role in stress redistribution. The underburden typically extends to greater depths and occupies a larger volume compared with the overburden in the modeled domain. As a result, it has a stronger capacity to accumulate and transmit elastic strain energy.

Furthermore, the stress response in the reservoir is influenced by the deformation compatibility between adjacent layers. Variations in the stiffness of the underburden can alter the strain partitioning between

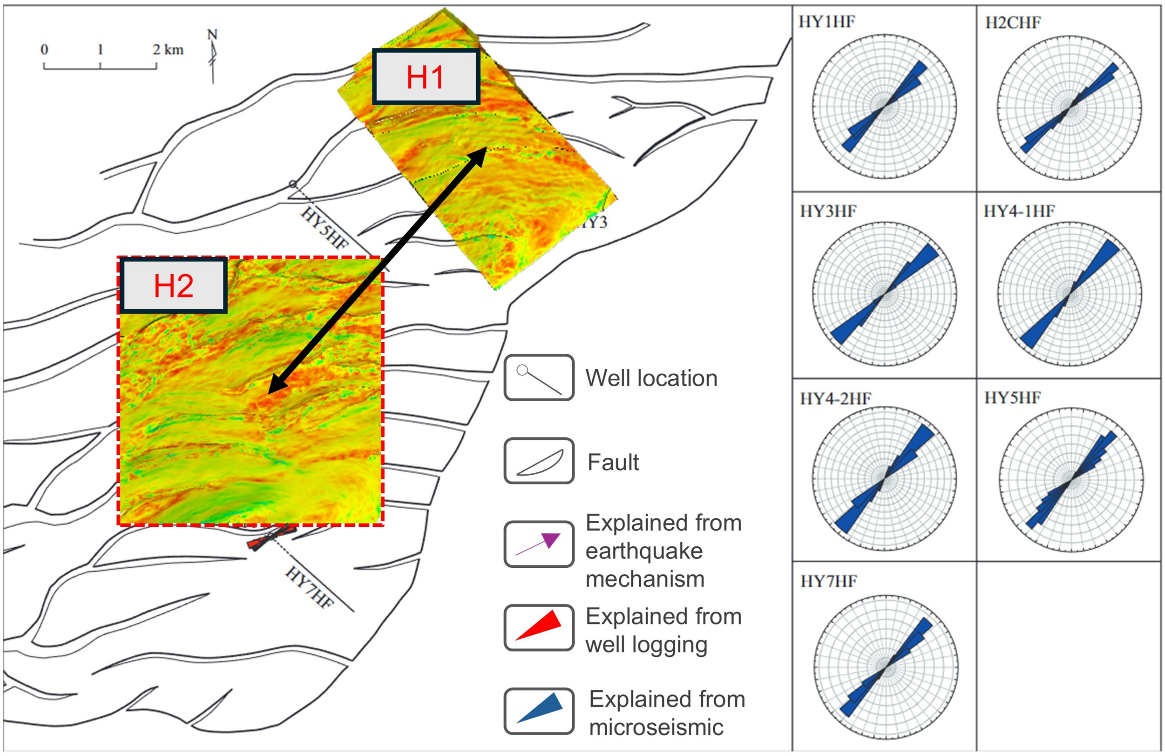

Figure 8. The left panel shows the locations of Block H1 and neighboring Block H2. The right panel shows the measured in-situ stress directions within the region.

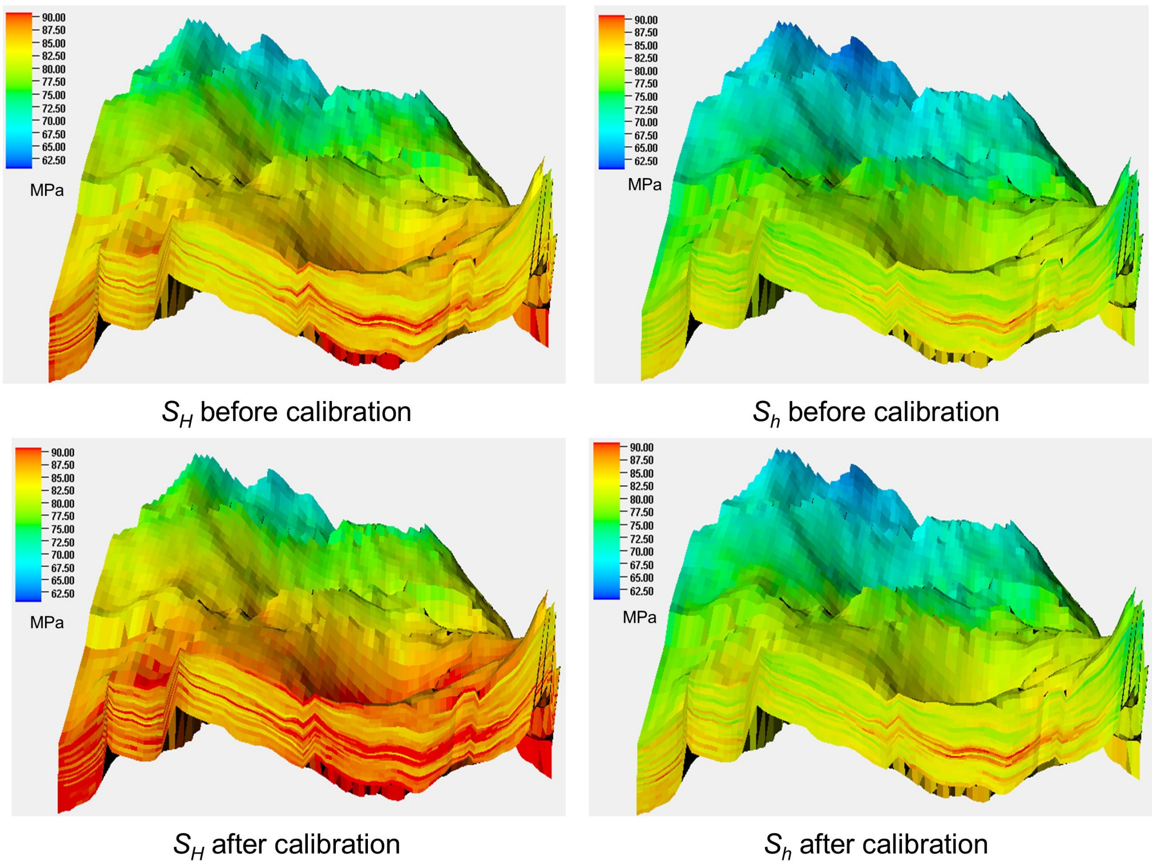

Figure 9. 3D stress distribution before and after single-step inversion calibration. S_H and S_h represent the simulated maximum and minimum horizontal principal stresses, respectively.

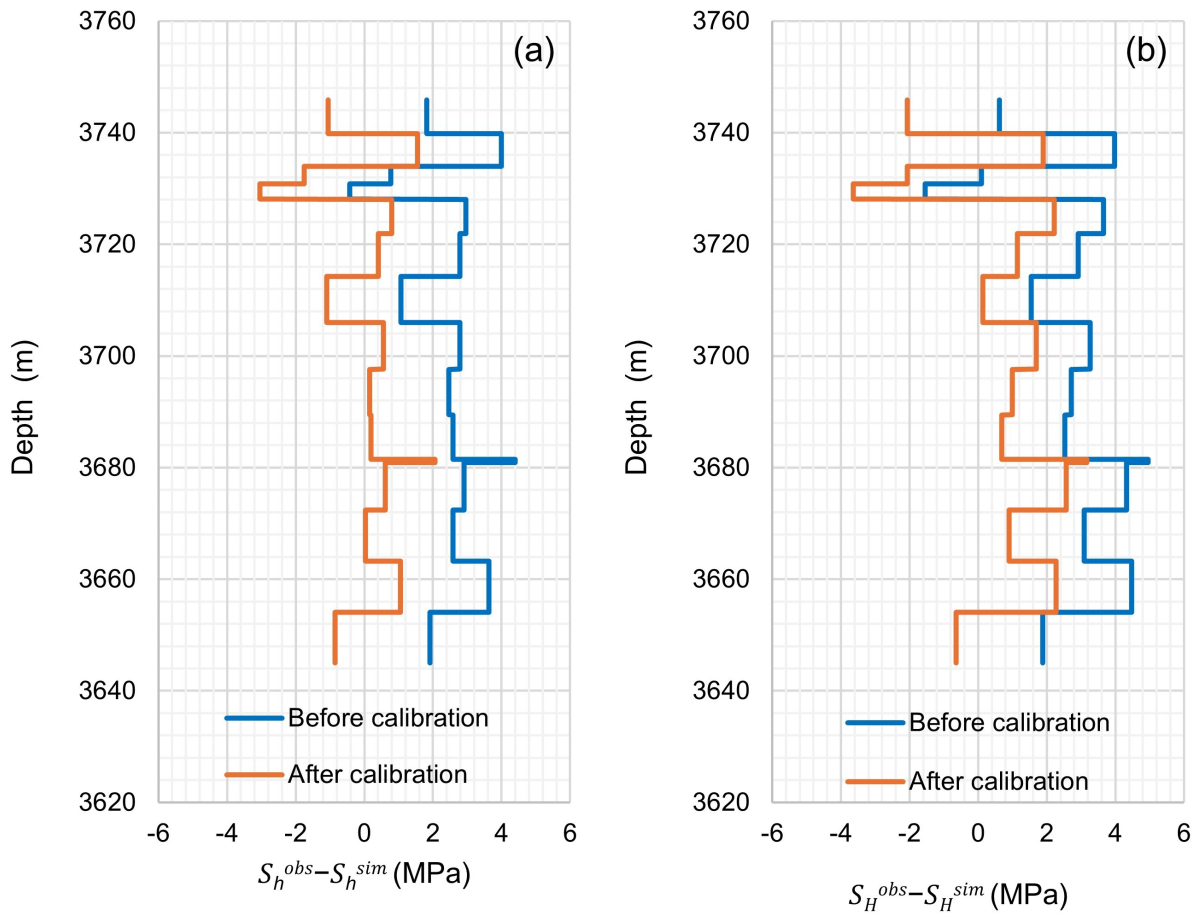

Figure 10. Depth-dependent residuals between the simulated and reference horizontal stresses before and after inversion calibration at a representative well in Block H2. Panels (a) and (b) show the residuals of S_h and S_H, respectively. The residual is defined as Sobs-Ssim. The blue and orange curves represent the results before and after calibration, respectively.

layers, leading to noticeable changes in horizontal stress magnitudes within the reservoir. In contrast, the overburden, although still influential, often contributes less due to its relatively smaller effective deformation volume within the modeled domain.

5.3 Applicability and Flexibility of Parameter Selection

A central feature of the proposed framework is its flexibility in parameter selection. Rather than prescribing a fixed set of inversion parameters, the method allows the parameter space to be adjusted according to data availability and geological conditions.

In many practical applications, the mechanical properties of the overburden can be reasonably constrained using logging data (e.g., sonic and density logs), laboratory measurements, or seismic inversion. Under such conditions, treating the overburden as a fixed input and focusing the inversion on the underburden provides a stable and efficient solution. This reduced-parameter strategy decreases the dimensionality of the inversion problem and improves interpretability without significantly compromising accuracy.

However, this simplification is not mandatory. When the mechanical properties of the overburden are uncertain or poorly constrained, it is more appropriate to include both overburden and underburden parameters in the inversion. In this case, the sensitivity matrix is expanded, and the inversion is performed using a least-squares or regularized formulation, following standard geophysical inverse theory.

This adaptive parameter selection strategy ensures that the proposed framework can be applied across a wide range of geological scenarios. It also reduces the risk of bias introduced by over-simplified parameter assumptions, thereby enhancing the robustness of the calibration process.

It should be noted that elastic-parameter updates obtained from stress inversion are conditional on the adopted geological structure, boundary conditions, and parameterization scheme. Different combinations of mechanical properties and boundary loading may produce similar stress responses. Therefore, the inverted parameters should be interpreted as effective calibration parameters for improving stress prediction rather than unique measurements of formation properties.

5.4 Validity and Limitations of Cross-block Sensitivity Transfer

The cross-block sensitivity transfer strategy is based on the assumption that sensitivity coefficients reflect intrinsic mechanical relationships controlled by stratigraphy and tectonic stress regime. When two blocks share similar geological conditions, these relationships are expected to remain approximately valid.

The present case demonstrates that an H1-derived sensitivity matrix can provide a useful first-order calibration basis for H2 under comparable geological and mechanical conditions. This may reduce the need for repeated sensitivity simulations and improves modeling efficiency. However, because an independently constructed sensitivity matrix for H2 was not evaluated, the present study demonstrates feasibility rather than universal transferability.

Nevertheless, the validity of this transfer is not universal. The approach may be less reliable under the following conditions: (1) strong lateral heterogeneity in lithology or thickness; (2) significant structural complexity, such as major faults or folds; (3) changes in tectonic stress regime. Under such conditions, the sensitivity relationships may deviate from those of the reference block, and recalibration of the sensitivity matrix may be required. Therefore, geological similarity should be carefully evaluated before applying cross-block transfer.

5.5 Assumptions and Limitations of the Inversion Framework

The proposed inversion framework relies on several simplifying assumptions, which are discussed below. First, the relationship between parameter perturbations and stress responses is approximated as linear. The sensitivity matrix represents a first-order approximation around the baseline model. Therefore, the proposed inversion is most suitable for moderate parameter variations where the local parameter–stress relationship remains approximately linear. It is important to note that non-linear or iterative extensions might be required when applying this method under extreme structural deformations or highly non-linear material behaviors. This assumption is generally valid for moderate parameter variations, as used in the sensitivity analysis. Second, the inversion is based on average stress responses within the reservoir. While this is sufficient for overall calibration, it may not capture localized stress variations associated with small-scale heterogeneity or discrete fractures. Third, the inversion problem may become underdetermined when multiple parameters are included simultaneously. Although regularization techniques can mitigate this issue, the solution may still depend on the choice of weighting factors. Despite these limitations, the framework provides a practical balance between model complexity and computational efficiency, making it suitable for many field-scale applications.

It should also be noted that the current application adopts an equivalent isotropic elastic representation at the block scale. Although shale formations commonly exhibit bedding-related anisotropy, continuous constraints on the complete anisotropic stiffness tensor were unavailable for the studied blocks. Therefore, the adopted elastic parameters represent upscaled effective properties. Future applications may incorporate directional elastic parameters into the sensitivity matrix when sufficient anisotropic measurements are available.

5.6 Implications for Geomechanical Modeling Practice

The results of this study have several implications for practical geomechanical modeling. First, the proposed framework suggests that when regional boundary conditions are independently constrained, adjusting effective mechanical properties of surrounding formations provides an alternative calibration pathway that avoids repeated empirical modification of the boundary loading. This shift helps maintain the physical consistency of the stress field and avoids artificial distortion of regional stress patterns. Second, the use of a sensitivity matrix enables rapid estimation of elastic parameter updates, reducing the need for iterative trial-and-error simulations. This is particularly beneficial in multi-well or multi-block modeling scenarios, where repeated calibration can be time-consuming. Third, the adaptive elastic parameter selection strategy provides a practical guideline for modelers: prioritize elastic parameters with high sensitivity and low data constraint, while fixing elastic parameters that are well constrained by measurements. Finally, the cross-block transfer concept offers a pathway toward more efficient regional modeling workflows, in which knowledge derived from mature blocks can be reused in newly developed areas.

6 Conclusions

The main conclusions of this study are summarized as follows:

A sensitivity-driven inversion framework is developed for efficient calibration of horizontal stresses in 3D geomechanical models. By separating the calculation of vertical stress from the calibration of horizontal stresses, the inversion problem is simplified while maintaining a clear physical basis.

A sensitivity matrix is constructed to quantify the relationship between elastic parameter variations and horizontal stress responses. This matrix enables direct estimation of elastic parameter updates, transforming conventional trial-and-error calibration into a quantitative first-order parameter-update procedure.

An adaptive elastic parameter selection strategy is proposed, in which inversion elastic parameters are selected based on sensitivity dominance and data availability. In cases where overburden properties are well constrained, the inversion can focus on the underburden; otherwise, both overburden and underburden elastic parameters can be included. This flexibility enhances the applicability and robustness of the framework.

A cross-block sensitivity transfer approach is introduced, suggesting that sensitivity relationships derived from a reference block may provide a useful first-order calibration basis for geologically similar neighboring blocks. This may reduce the need for repeated sensitivity analysis and improves modeling efficiency.

Application to a shale reservoir case demonstrates that the proposed method can effectively reduce stress prediction errors. The calibration requires only one inversion step and one forward simulation after the sensitivity matrix has been established, in contrast to conventional trial-and-error procedures that typically require multiple iterations. The results suggest that the framework provides a practical alternative to conventional empirical calibration methods.

Data Availability Statement

Data will be made available on request.

Funding

This work was supported by the Sinopec Science and Technology Research Project under Grant P25129 and Grant P24219.

Conflicts of Interest

Hao Wu, Xinrui Lyu, and Xiaofei Shang are affiliated with the SINOPEC Petroleum Exploration and Production Research Institute, Beijing 102206, China; Xiaokai Huang is affiliated with the Petroleum Engineering Technology Research Institute, Sinopec Jiangsu Oilfield Company, Yangzhou 225009, China. The authors declare that these affiliations had no influence on the study design, data collection, analysis, interpretation, or the decision to publish, and that no other competing interests exist.

AI Use Statement

The authors declare that no generative AI was used in the preparation of this manuscript.

Ethical Approval and Consent to Participate

Not applicable.

References

[1] Boak, J., & Kleinberg, R. (2020). Shale gas, tight oil, shale oil and hydraulic fracturing. In *Future Energy* (pp. 67–95). Elsevier. [CrossRef]

[2] Guo, X., Shen, B., Li, M., Liu, H., Li, Z., Zhang, S., Yang, Y., Guo, J., Liu, Y., & Li, P. (2025). Research progress and key research directions of shale oil in lacustrine rift basins. *Petroleum Exploration and Development*, *52*(5), 1113–1127. [CrossRef]

[3] Sun, H., Lv, Q., Fang, J., Lü, J., Zhu, Y., & Qian, K. (2025). Development technology and direction of shale oil in continental rift basins. *Acta Petrolei Sinica*, *46*(8), 1589–1601. [CrossRef]

[4] Yin, S., Xie, J. Y., Cheng, L. L., Wu, Y. X., Zhu, B. Y., & Chen, G. Y. (2022). Advances in continental shale oil research and problems of reservoir geology. *Acta Sedimentologica Sinica*, *40*, 979–995. http://www.cjxb.ac.cn/en/article/doi/10.14027/j.issn.1000-0550.2021.109

[5] Caineng, Z. O. U., Zhi, Y. A. N. G., Jingwei, C. U. I., Rukai, Z., Lianhua, H., Shizhen, T.,

... & Jingli, Y. (2013). Formation mechanism, geological characteristics and development strategy of nonmarine shale oil in China. *Petroleum exploration and development*, *40*(1), 15-27. [CrossRef]

[6] Zhijun, J. I. N., Rukai, Z. H. U., & Yunqi, S. H. E. N. (2021). Several issues worthy of attention in current lacustrine shale oil exploration and development. *Petroleum Exploration and Development*, *48*(6), 1471-1484. [CrossRef]

[7] Suyun, H. U., Wenzhi, Z. H. A. O., Lianhua, H. O. U., Zhi, Y., Rukai, Z., Songtao, W., ... & Xu, J. (2020). Development potential and technical strategy of continental shale oil in China. *Petroleum Exploration and Development*, *47*(4), 877-887. [CrossRef]

[8] Feng, Q., Xu, S., Xing, X., Zhang, W., & Wang, S. (2020). Advances and challenges in shale oil development: A critical review. *Advances in Geo-Energy Research*, *4*(4), 406-418. [CrossRef]

[9] Cipolla, C. L., Warpinski, N. R., Mayerhofer, M. J., Lolon, E. P., & Vincent, M. C. (2010). The relationship between fracture complexity, reservoir properties, and fracture-treatment design. *SPE production & Operations*, *25*(04), 438-452. [CrossRef]

[10] Mayerhofer, M. J., Lolon, E. P., Warpinski, N. R., Cipolla, C. L., Walser, D., & Rightmire, C. M. (2010). What is stimulated reservoir volume?. *SPE Production & Operations*, *25*(01), 89-98. [CrossRef]

[11] Zhang, Y., Zhang, J., Yuan, B., & Yin, S. (2018). In-situ stresses controlling hydraulic fracture propagation and fracture breakdown pressure. *Journal of Petroleum Science and Engineering*, *164*, 164-173. [CrossRef]

[12] Nasehi, M. J., & Mortazavi, A. (2013). Effects of in-situ stress regime and intact rock strength parameters on the hydraulic fracturing. *Journal of Petroleum Science and Engineering*, *108*, 211-221. [CrossRef]

[13] Zhang, Y., Wei, S., Jin, Y., & Wang, D. (2024). 3D Dynamic Stress Evolution of the Continental Shale Oil Reservoirs. *Chinese Journal of Underground Space and Engineering*, *20*, 163–171. https://dxkjxb.cqu.edu.cn/EN/10.20174/j.JUSE.2024.S1.20

[14] Xiao, Y., Liang, C., Zhu, D., Zou, C., Yan, J., & Bai, Y. (2024). Multi-Scale Geomechanical Modelling of Unconventional Shale Gas: The Implication on Assisting Geophysics–Geology–Engineering Integration. *International Journal of Energy Research*, *2024*(1), 4145930. [CrossRef]

[15] Xiao, Y., Jiang, W., & Liang, C. (2024). Data-driven multiscale geomechanical modeling of unconventional shale gas reservoirs: a case study of Duvernay Formation, Alberta, West Canadian Basin. *Frontiers in Earth Science*, *12*, 1437255. [CrossRef]

[16] Liu, J., Ding, W., Yang, H., Wang, R., Yin, S., Li, A., & Fu, F. (2017). 3D geomechanical modeling and numerical simulation of in-situ stress fields in shale reservoirs: a case study of the lower Cambrian Niutitang formation in the Cen'gong block, South China. *Tectonophysics*, *712*, 663-683. [CrossRef]

[17] Hergert, T., Heidbach, O., Reiter, K., Giger, S. B., & Marschall, P. (2015). Stress field sensitivity analysis in a sedimentary sequence of the Alpine foreland, northern Switzerland. *Solid Earth*, *6*(2), 533-552. [CrossRef]

[18] Li, H., Wang, G., Pang, X., Liu, X., Wang, G., Shu, H., Luo, Y., Liu, M., & Lai, J. (2023). Logging evaluation of the engineering quality of the Paleogene Funing Formation oil shales in the Subei Basin. *Bulletin of Geological Science and Technology*, *42*(3), 311–322. [CrossRef]

[19] Hou, S. Y., Wang, X. Q., Xian, C. G., Ge, H., & Zhong, Y. (2026). Research on high-precision one-dimensional geomechanical modeling of shale oil reservoirs. *Journal of Geomechanics*, *32*(2), 353–364. [CrossRef]

[20] Markou, N., & Papanastasiou, P. (2025). 3D Geomechanical Finite Element Analysis for a Deepwater Faulted Reservoir in the Eastern Mediterranean: N. Markou, P. Papanastasiou. *Rock Mechanics and Rock Engineering*, *58*(1), 65-86. [CrossRef]

[21] Liu, Q., Fu, Q., Yang, K., Wei, Q., Liu, H., & Wu, H. (2022). Geomechanical modeling and inversion Analysis of the in-situ stress field in deep marine shale formations: A case study of the Longmaxi Formation, Dingshan Area, China. *Frontiers in Earth Science*, *9*, 808535. [CrossRef]

[22] Chen, Y., Li, W., Wang, X., Wang, Y., Fu, L., Wu, P., & Wang, Z. (2025). Research and Application of Geomechanics Using 3D Model of Deep Shale Gas in Luzhou Block, Sichuan Basin, Southwest China. *Geosciences*, *15*(2), 65. [CrossRef]

[23] Chen, P., Qiu, H., Chen, X., & Shen, C. (2024). Refined 3D numerical simulation of in situ stress in shale reservoirs: Northern Mahu Sag, Junggar basin, Northwest China. *Applied Sciences*, *14*(17), 7644. [CrossRef]

[24] Rybacki, E., Reinicke, A., Meier, T., Makasi, M., & Dresen, G. (2015). What controls the mechanical properties of shale rocks?–Part I: Strength and Young's modulus. *Journal of Petroleum Science and Engineering*, *135*, 702-722. [CrossRef]

[25] Sone, H., & Zoback, M. D. (2013). Mechanical properties of shale-gas reservoir rocks—Part 1: Static and dynamic elastic properties and anisotropy. *Geophysics*, *78*(5), D381-D392. [CrossRef]

[26] Gao, H., Gao, Y., He, X., & Nie, J. (2024). Rock mechanical properties and controlling factors for shale oil reservoirs in the second member of the Paleogene Funing Formation, Subei Basin. *Oil & Gas Geology*, *45*(2), 502–515. [CrossRef]

[27] Sayers, C. M. (2013). The effect of kerogen on the elastic anisotropy of organic-rich shales. *Geophysics*, *78*(2), D65-D74. [CrossRef]

[28] Labani, M. M., & Rezaee, R. (2015). The importance

of geochemical parameters and shale composition on rock mechanical properties of gas shale reservoirs: A case study from the Kockatea Shale and Carynginia Formation from the Perth Basin, Western Australia. *Rock Mechanics and Rock Engineering*, *48*(3), 1249-1257. [CrossRef]

[29] Tuzingila, R. M., Kong, L., & Kasongo, R. K. (2024). A review on experimental techniques and their applications in the effects of mineral content on geomechanical properties of reservoir shale rock. *Rock Mechanics Bulletin*, *3*(2), 100110. [CrossRef]

[30] Xiong, J., Gan, R., Liu, X., Liang, L., & Guo, X. (2023). Evaluation of the rock mechanical properties of shale oil reservoirs: A case study of Permian Lucaogou Formation in the Jimusar sag, Junggar Basin. *Applied Sciences*, *13*(23), 12851. [CrossRef]

[31] Houbin, L. I. U., Shuang, W. A. N. G., Shuang, D. U., Xinjie, L. I., & Chengjin, L. E. N. G. (2025). Dynamic evolution law of in-situ stress field in fractured shale reservoirs. *Petroleum Drilling Techniques*, *53*(4), 85-93. [CrossRef]

[32] Cui, S., Wu, J., Zeng, B., Huang, H., Wang, S., Liu, H., & Gui, J. (2025). Study on the evolution law of four-dimensional in situ stress during hydraulic fracturing of deep shale gas reservoir. *Processes*, *13*(12), 3772. [CrossRef]

[33] Fischer, K., & Henk, A. (2013). A workflow for building and calibrating 3-D geomechanical models &ndash a case study for a gas reservoir in the North German Basin. *Solid Earth*, *4*(2), 347-355. [CrossRef]

[34] Duan, H., Sun, Y., & Yang, B. (2024). Main controlling factors of shale oil enrichment in second member of Paleogene Funing Formation in Gaoyou Sag of Subei Basin. *Petroleum Geology* & *Experiment*, *46*(3), 441–450. [CrossRef]

[35] Huang, X., Huang, Y., Jin, Z., & He, L. (2026). Research on key fracturing technology for deep shale oil in Gaoyou Sag, Subei Basin. *Petroleum Reservoir Evaluation and Development*, *16*(2), 443-450. https://www.pred.com.cn/en/article/doi/10.13809/j.cnki.cn32-1825/te.2024389/

[36] Yan, Z., Liang, B., Sun, Y., Duan, H., & Qiu, X. (2024). In-situ stress orientation and main controlling factors of deep shale reservoirs in the second member of Paleogene Funing Formation in Gaoyou Sag, Subei Basin. *Experimental Petroleum Geology*, *46*(6), 1187-1197. [CrossRef]

[37] Li, P., Liu, Z., Duan, H., Ge, X., & Nie, H. (2024). Controlling Factors of Shale Oil Enrichment in the Paleogene Funing Formation, Gaoyou Sag, Subei Basin, China. *Energy* & *Fuels*, *38*(19), 18521-18532. [CrossRef]

[38] Zoback, M. D. (2007). *Reservoir geomechanics*. Cambridge University Press. [CrossRef]

[39] Zoback, M. D., & Kohli, A. H. (2019). *Unconventional reservoir geomechanics: Shale gas, tight oil, and induced seismicity*. Cambridge University Press. [CrossRef]